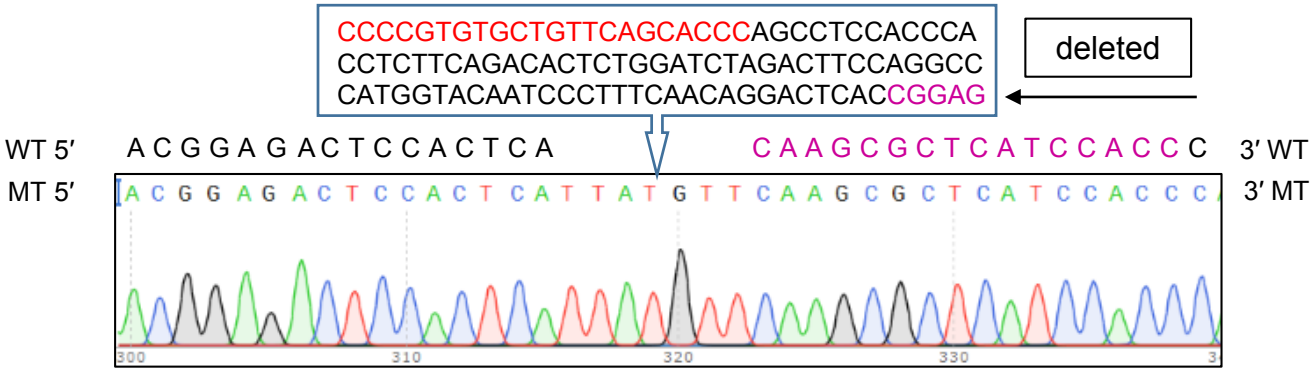

Ngf Guide sequence 1 (reverse complement): CCCGTGTGCTGTTCAGCACCC
Guide sequence 2 (reverse complement): CGGAGCAAGCGCTCATCCACC

Supplementary Figure 1 A 104-nt deletion in the *Ngf* gene is caused by the expression of two sgRNAs and SaCas9. Mouse CD45$^-$ BMSCs were transfected with two individual px601 vectors, within which two sgRNAs targeting different loci (marked with purple and red respectively) of the *Ngf* gene were expressed. The genomic DNA was extracted from the transfected cells and the related region was amplified and sequenced to show that these two sgRNAs effectively targeted two loci of the *Ngf*, resulting in a 104-nt deletion of the gene and a loss-of-function of the NGF protein. WT, wildtype; MT, mutant.

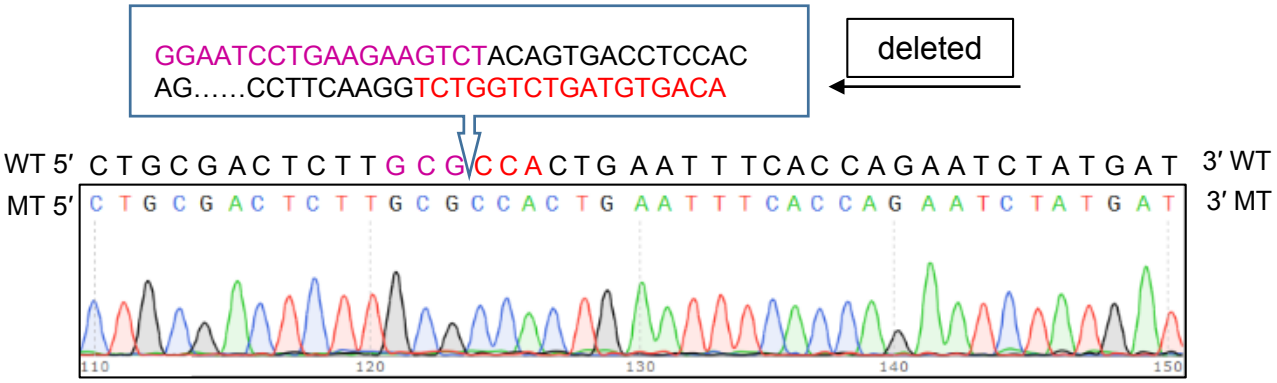

Mmp13 Guide sequence 1 reverse complement : GCGGGAATCCTGAAGAAGTCT
Guide Sequence 2: TCTGGTCTGATGTGACACCA

Supplementary Figure 2 A 1174-nt deletion in the *Mmp13* gene is caused by the expression of two sgRNAs and SaCas9. Note that most nucleotides within the deleted sequence are omitted for brevity.

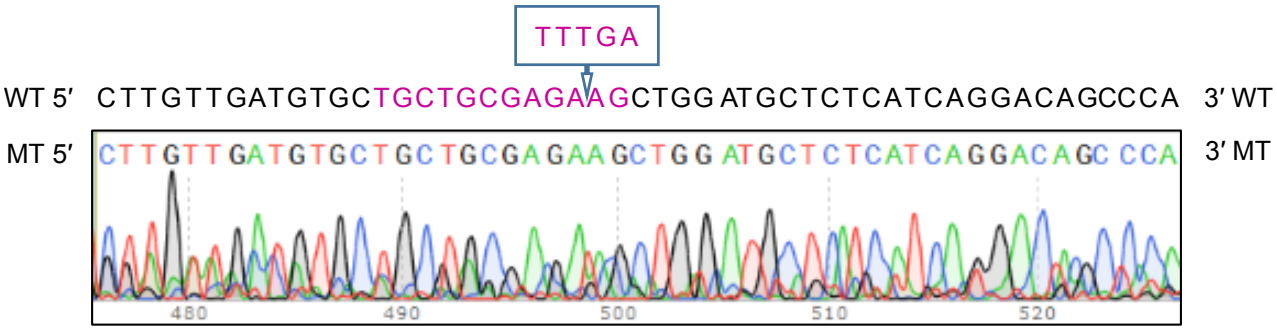

IL-1β Guide sequence 1: TGCTGCTGCGAGATTTGAAG

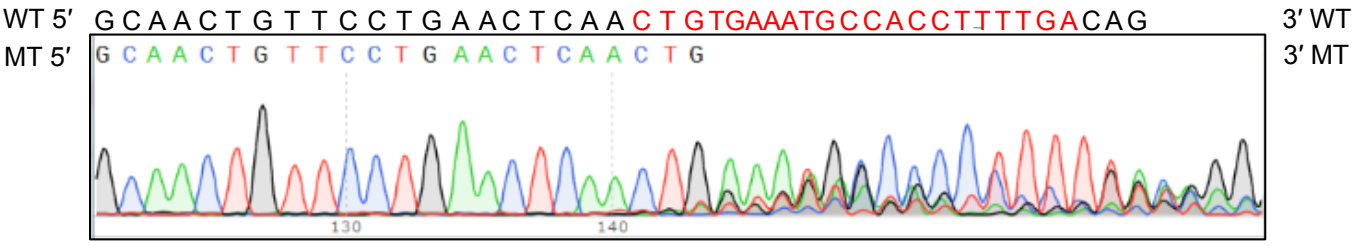

IL-1β Guide sequence 2 reverse complement: CTGTGAAATGCCACCTTTTGA

Supplementary Figure 3 Two sgRNAs for IL-1β caused indels. For *IL-1β* sgRNA 1, a 5-nt deletion is generated; for sgRNA 2, double peaks can be seen starting from the last fourth nt of the guide sequence, indicating that the DNAs are heterogeneous and thus contain mutants.

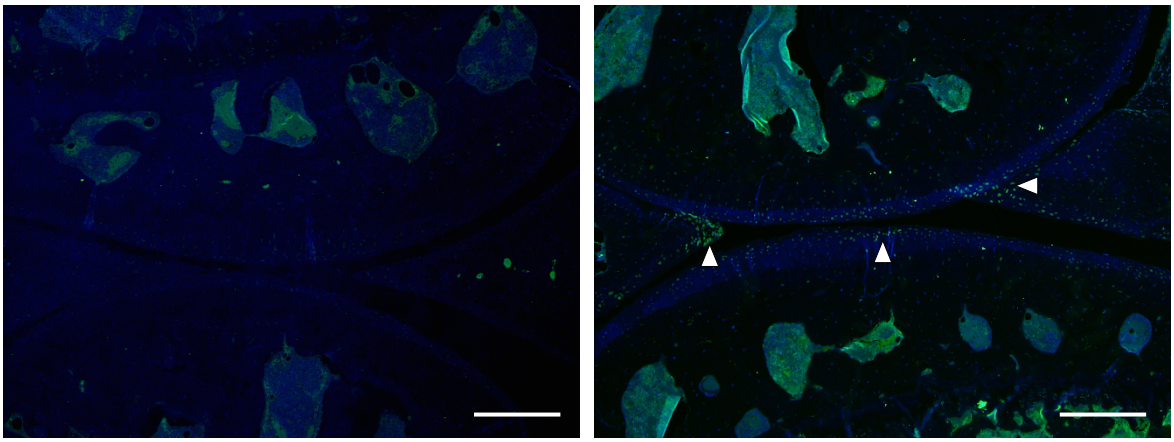

Supplementary Figure 4 Immunofluorescence (IF) of GFP expression in joint tissues after AAV5-GFP administration. IF data showed GFP expression in the knee joints of 6-month-old C57BL/6 mice that received AAV5-GFP or control AAV injections at the age of 3 months. n = 5. Arrowheads, GFP-positive cells. Scale bar: 200 μm.

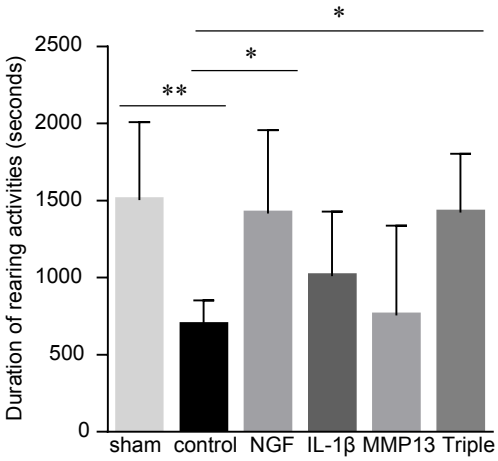

Supplementary Figure 5 The duration of rearing of the mice were measured on the Laboratory Animal Behaviour Observation, Registration and Analysis System (LABORAS). All groups except sham received the OA-inducing PMM surgery and injections of gene-targeting AAV as indicated. n = 7. * $p < 0.05$, ** $p < 0.01$. One-way ANOVA followed by the Tukey-Kramer test.

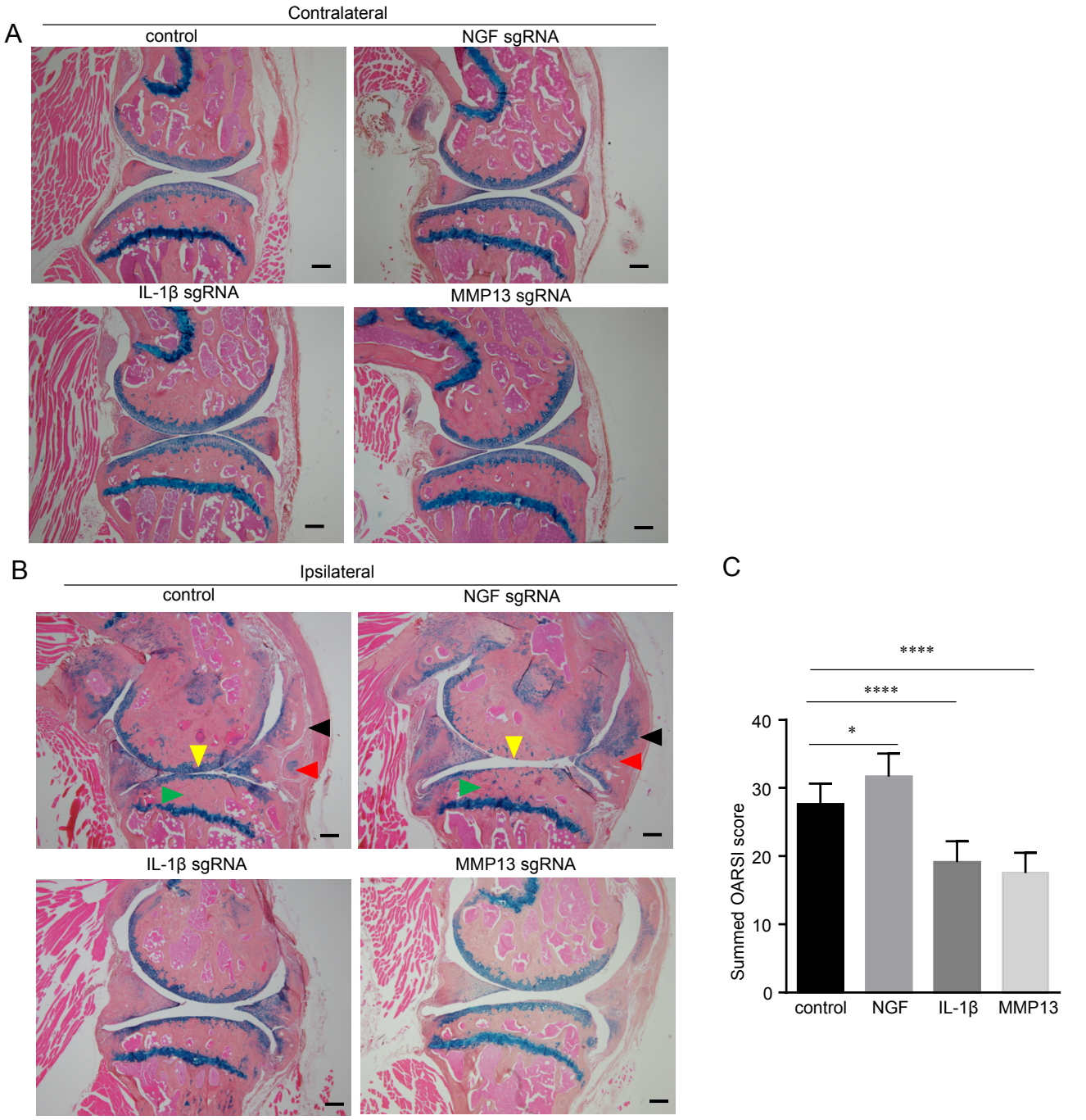

Supplementary Figure 6 OA-modifying effects by CRISPR-mediated ablation of NGF, IL-1β, and MMP13. (A) CRISPR-mediated gene ablation on the ipsilateral (operated and AAV-injected) knees did not change the histologic morphology of the contralateral (unoperated and unjected) knee joints. (B) Representative histology images of osteoarthritic knee joints, which were collected six months after injections of indicated AAVs. Yellow arrowheads, loss of articular cartilage; red arrowheads, osteochondrophytes; black arrowheads, synovial hyperplasia; green arrowheads, subchondral sclerosis. Scale bar, 200 μm. (C) OARSI scoring of knee joint articular cartilage destruction in the mice receiving the PMM surgery and control or gene-targeting AAV. Both medial femoral condyle and medial tibial plateau were analyzed on three-level sections of the joints and summed OARSI scores for the entire joint were presented. *p<0.05, ****p<0.0001. One-way ANOVA, n = 9.

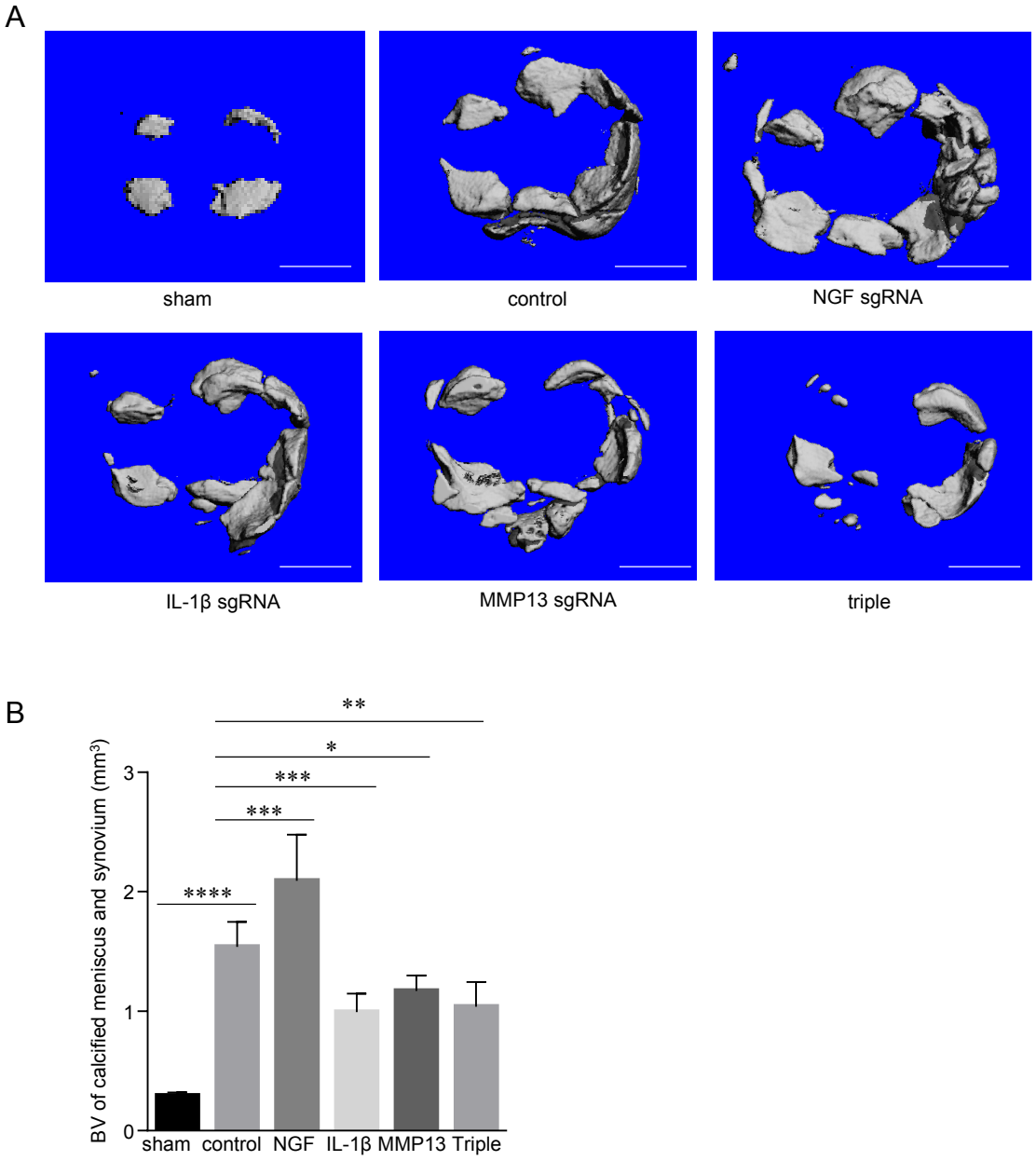

Supplementary Figure 7 μCT analysis and quantification of ectopic bone formation around meniscus and synovium in osteoarthritic knee joints. (A and B) Representative μCT images (A) and bone volume (BV) quantification (B) of calcified meniscus and synovium in osteoarthritic knee joints, which were collected six months after injections of control, NGF-, IL-1β, MMP13, or triple (NGF, IL-1β and MMP13)-targeting AAVs. Scale bar for μCT, 1 mm. n = 6. One-way ANOVA followed by the Tukey-Kramer test. *p<0.05, **p<0.01, ***p<0.001, ****p<0.0001.

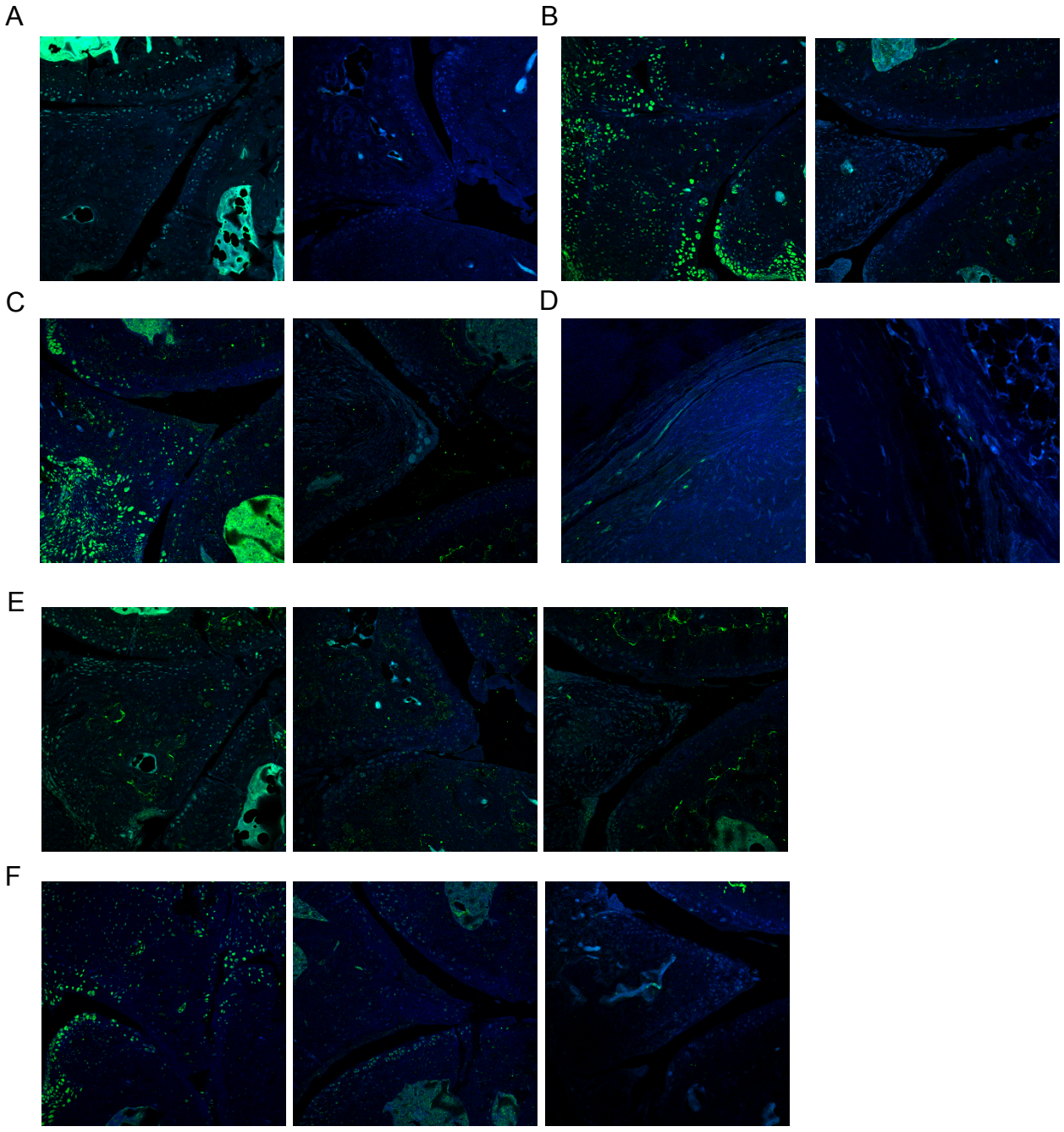

Supplementary Figure 8 Fluorescence-based IHC Images with DAPI signals merged were shown to assist the evaluation of tissue distribution in the IHC analysis related to Figure 2. The labels (A-F) are exactly corresponding to those in Figure 2. Except the IHC for βIII Tubulin (D) that analysed synovium, all figures focus on the areas that show meniscus (the triangle-like shapes), synovium, femoral and tibial cartilage together.

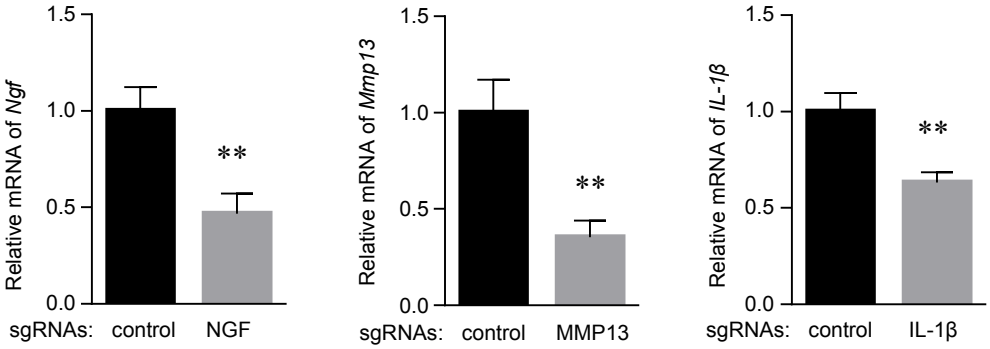

Supplementary Figure 9 Quantitative RT-PCR analysis of *Ngf, Mmp13,* and *IL-1β* expression in the knee joint receiving injections of control, NGF-, MMP13-, IL-1β-targeting AAVs. ** $p < 0.01$, unpaired Student's *t*-test. n = 3.

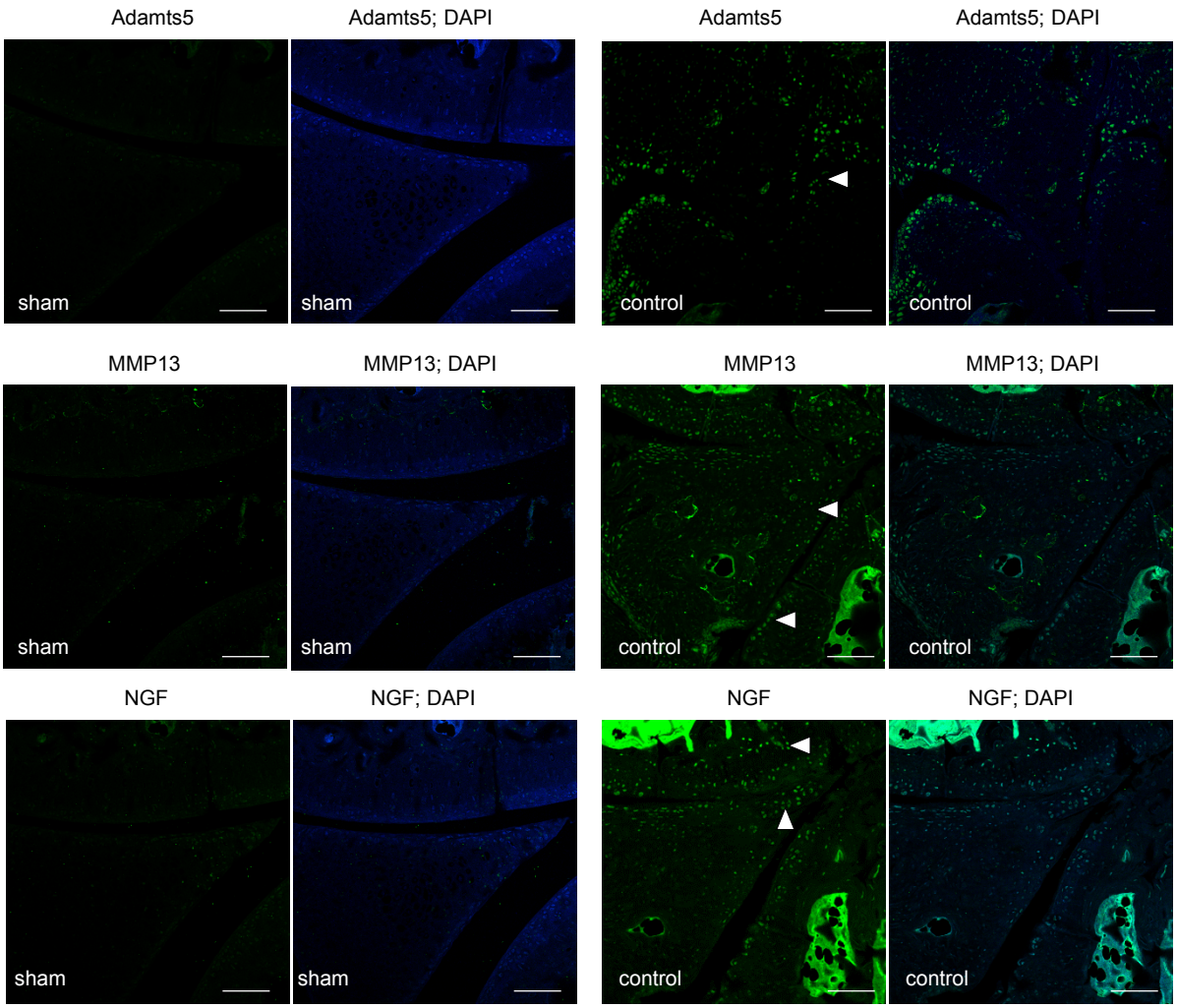

Supplementary Figure 10 Fluorescent IHC of Adamts5, MMP13, and NGF in the sham joints, which did not receive meniscectomy and therefore did not develop PTOA. In order to compare the sham data with the control (operated) group, figures for the control group used in Figure 2 and Supplementary Figure 8 are displayed in the right panels. n = 5. Arrowheads, IHC-positive signals. Scale bar: 50 μm.

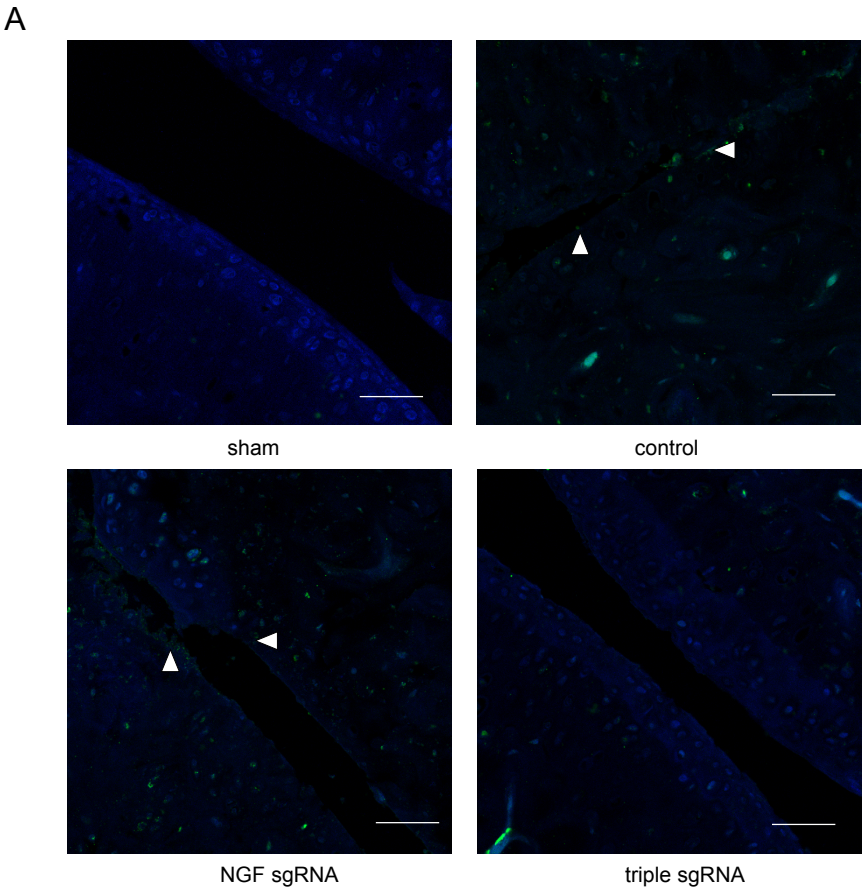

Supplementary Figure 11 Immunofluorescence of a neoepitope (NITEGE) of Aggrecan, a degradation product of Aggrecan in the knee joints receiving the surgery and gene-targeting AAVs as indicated. (A) Representative images of the immunofluorescence results. Arrowheads, neoepitope-positive signals. Scale bar: 25 μm. (B) Quantification of relative neoepitope-positive fluorescence intensity among the samples. n = 4. *p<0.05, **p<0.01, ***p<0.001. One way ANOVA.

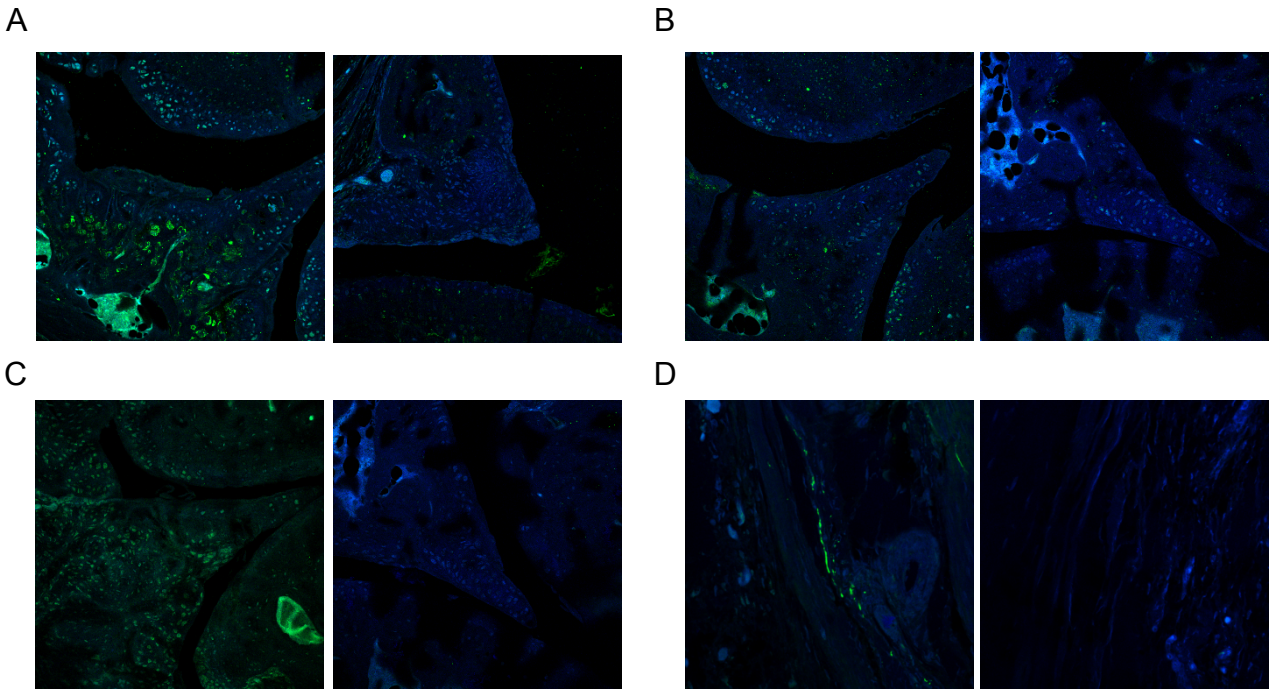

Supplemental Figure 12 Fluorescence-based IHC Images with DAPI signals merged were shown to assist the evaluation of tissue distribution in the IHC analysis related to Figure 3. The labels (A-D) are corresponding to Figures 3F-I in alphabetical order. Except the IHC for βIII Tubulin (D) that analysed synovium, all figures focus on the areas that show meniscus (the triangle-like shapes), synovium, femoral and tibial cartilage together.